

Measuring the angle-dependent photoionization cross section of nitrogen using high-harmonic generation

Xiaoming Ren,¹ Varun Makhija,¹ Anh-Thu Le,¹ Jan Troß,^{1,2} Sudipta Mondal,¹ Cheng Jin,¹
Vinod Kumarappan,^{1,*} and Carlos Trallero-Herrero^{1,†}

¹*J. R. Macdonald Laboratory, Kansas State University, Manhattan, Kansas 66506, USA*

²*Institut für Kernphysik, Johann Wolfgang Goethe Universität Frankfurt, 60438 Frankfurt, Germany*

(Received 16 April 2013; published 17 October 2013)

We exploit the relationship between high harmonic generation (HHG) and the molecular photorecombination dipole to extract the molecular-frame differential photoionization cross section (PICS) in the extreme ultraviolet (XUV) for molecular nitrogen. A shape resonance and a Cooper-type minimum are reflected in the pump-probe time delay measurements of different harmonic orders, where high-order rotational revivals are observed in N₂. We observe the energy- and angle-dependent Cooper minimum and shape resonance directly in the laboratory-frame HHG yield by achieving a high degree of alignment, $\langle \cos^2 \theta \rangle \geq 0.8$. The interplay between PICS and rotational revivals is confirmed by simulations using the quantitative rescattering theory. Our method of extracting molecular-frame structural information points the way to similar measurements in more complex molecules.

DOI: [10.1103/PhysRevA.88.043421](https://doi.org/10.1103/PhysRevA.88.043421)

PACS number(s): 33.80.Eh, 42.50.Hz, 33.15.Bh, 42.65.Re

I. INTRODUCTION

Although extreme ultraviolet (XUV) photoionization [1] is a powerful and well-established tool for studying molecular properties, it suffers from some shortcomings. Experiments have to be performed in large synchrotron facilities and—without aligning the molecules—molecular-frame measurements are not possible for states that do not fragment upon ionization. As first proposed in Refs. [2,3], high harmonic generation (HHG) spectra contain information about target molecular structure. According to the quantitative rescattering (QRS) theory [4,5], the relation between HHG and photoionization cross section (PICS) can be exploited to overcome these difficulties. This approach can be intuitively understood based on a simple semiclassical picture of the HHG process: (1) An electron tunnels through the barrier that the electric field has lowered; (2) once in the continuum it gains energy from the field; and (3) as the laser electric field reverses direction and drives it back to the parent molecular ion, there is a finite probability for photorecombination with the emission of an XUV photon [6,7]. This process depends on the angle between the laser polarization vector and the molecular axis. When combined with field-free molecular axis alignment, HHG thus promises to become a formidable tool for the study of time-, angle-, and energy-resolved molecular structure [2,8,9]. Unlike traditional XUV sources, HHG can be driven by femtosecond pulses in pump-probe configurations for dynamical studies. In fact, HHG spectroscopy has already been used to reveal static molecular structures [2,9–16] as well as dynamics features [8,17–21]. Furthermore, it has also been demonstrated that the relationship between PICS and HHG is maintained even in the presence of multielectron correlations [22].

In this paper, we report the measurement of high-order rotational revivals in the HHG signal from N₂ and show that

the detailed revival pattern reflects the angle dependence of the PICS, which we extract from this time-domain measurement. The well-known $3\sigma_g \rightarrow k\sigma_u$ shape resonance, which is localized at $\theta \leq 30^\circ$ and occurs around 30 eV photon energy, and a Cooper-like minimum near 50 eV are both seen in the extracted PICS. This method is an alternative to those demonstrated in Refs. [16,23] with the advantage that it can be extended to asymmetric top molecules since no angle scans are necessary. We also show that angular measurements made at the peak of alignment show these features of the PICS directly in the data without the need for deconvolution of the molecular axis distribution. The delay and angle measurements yield similar results in spite of the differences in the analysis and approximations required; these experimental results agree with simulations using QRS, confirming our interpretation of the experimental data. Our results show the robustness of using HHG as an inverse photoionization experiment and open the door to the extension of these techniques to larger, more complex molecules.

II. DELAY-DEPENDENT HARMONIC YIELDS: THE INTERPLAY BETWEEN PICS AND ROTATIONAL REVIVALS

Our experimental setup is shown in Fig. 1. Pulses from the Kansas Light Source laser (2-mJ/pulse, 780-nm center wavelength, 30-fs pulse duration, 2-kHz repetition rate) are split into two with a broadband 70:30 (reflectance to transmission, R:T) beamsplitter. The reflected pulse is further split by a 60:40 beamsplitter to form the two pump pulses, while the transmitted pulse serves as the probe. The probe can be delayed with respect to the pump pulses by a computer-controlled translation stage; the delay between the two pump pulses is controlled by a manual delay stage and optimized to obtain the highest degree of alignment. Achromatic zero-order half-wave plates in the paths of all the beams allow independent control of all polarizations. The beams are then focused noncollinearly into a vacuum chamber by a single 35-cm focal length lens.

*vinod@phys.ksu.edu

†trallero@phys.ksu.edu

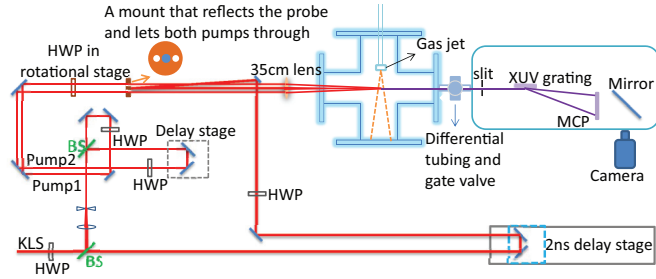


FIG. 1. (Color online) Experimental setup; see text for details.

A telescope located before the 60:40 beamsplitter allows for small adjustments to the focus of the pump beams relative to that of the probe beam. It also reduces the unfocused beam size to half that of the probe beam, thus ensuring a larger focal spot size for the pumps and harmonic generation only from aligned molecules. A 1 kHz Even-Lavie valve [24] produces a rotationally cold (~ 30 K) target by supersonic expansion of 70 bar of N_2 into the vacuum chamber; the interaction region is ~ 1 mm away from the nozzle. An XUV spectrometer—consisting of a 1-mm slit, a grazing incidence flat-field grating, a microchannel plate with a phosphor screen, and a 12-bit camera—is used to record the HHG spectrum. No attempt was made to calibrate the detection efficiency of the spectrometer. To avoid errors in the measured photon energy, the spectrum is calibrated with plasma emission lines from helium and neon gases [25]. By varying the focus of the probe pulse relative to the location of the gas jet, the phase matching of the HHG was adjusted to maximize the cutoff harmonics. In this condition, probe is focused about 3.5 mm before the jet with peak intensity estimated to be 250 TW/cm^2 .

In Fig. 2, the measured pump-probe harmonic signals are shown. The dip near 4 ps is due to increased ionization when the probe and the second pump overlap. The second pump arrives slightly before half-revival (rotational period of N_2 is 8.3 ps) due to the first pump; this delay was optimized to maximize the alignment immediately after the second pump. To estimate the degree of alignment, we solve the rigid rotor time-dependent Schrödinger equation for the rotational wave packet for a set of input parameters (intensities and pulse durations for the pumps and the rotational temperature). We then expand the measured amplitude of the 19th harmonic (H19) in a Legendre series, $\sqrt{S_{H19}(t)} = \sum_{J=0}^{J=4} a_{2J} \langle P_{2J}(\cos \theta) \rangle$ and determine the coefficients a_{2J} using a Levenberg-Marquadt nonlinear curve-fitting routine. The laser parameters and temperature are varied, and the fitting procedure is repeated to find the lowest mean-squared error between the data and the fit. The laser parameters and the temperature obtained from this procedure are then fixed and used to fit all the other harmonics by varying only the a_{2J} s. The best fit curves are also shown in Fig. 2. This fitting procedure allows us to extract both the molecular axis distribution (through the pump laser parameters) and the angle dependence of HHG in a manner similar to Ref. [26]. The angle dependence of the harmonics is shown in Fig. 3. The maximum alignment level at the full revival after the second pump, as estimated from the fit, is $\langle \cos^2 \theta \rangle \approx 0.82$. To the best of our knowledge, this is the tightest alignment achieved in an HHG experiment. In the

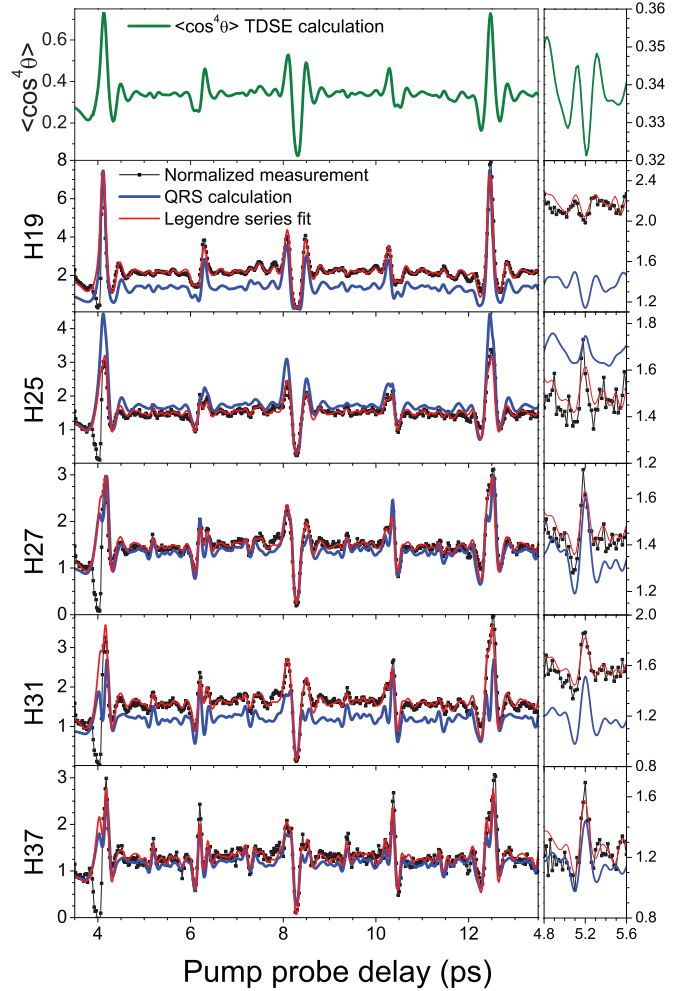


FIG. 2. (Color online) Experimental revival scans (black dots) are shown for harmonic orders 19, 25, 27, 31, and 37, all normalized to the corresponding isotropic signals. Laser parameters were obtained from the fit and used in the QRS calculations: the first pump is 80 fs FWHM with the peak at 0 ps, 48 TW/cm^2 ; the second pump is 80 fs, 56 TW/cm^2 ; separation between pump pulses is 3.94 ps; probe is 30 fs, 250 TW/cm^2 ; and the rotational temperature is 30 K.

top panel of Fig. 2 we also show $\langle \cos^4 \theta \rangle(t)$, the dominant term in the revival pattern for the highest occupied molecular orbital (HOMO) of N_2 according to Refs. [27,28].

Due to the strong alignment and to the sensitivity of HHG to the high-order moments of the angular distribution [28], fractional revivals at $1/8$ th of the rotational period can be seen in the data. It can also be clearly seen that the revival structure, including the incoherent alignment offset [29], varies with harmonic order. In particular, with increasing harmonic order the structure of the half revival (near 8 ps) becomes sharper, the $1/4$ th (near 6 ps), $3/4$ th (near 10 ps), and full (near 12 ps) revivals begin to split near the peak, and the direction of the $1/8$ th (near 5.2 ps, see insets of Fig. 2) revivals reverses around H21. These features show that higher order terms ($n > 2$) in $(\sum_n C_n \cos^{2n} \theta)^2$ cannot be neglected. The cutoff harmonics show particularly strong departure from a $\langle \cos^4 \theta \rangle$ distribution. In light of the quantitative rescattering (QRS) theory [4,30], we attribute these newly revealed features to the energy- and

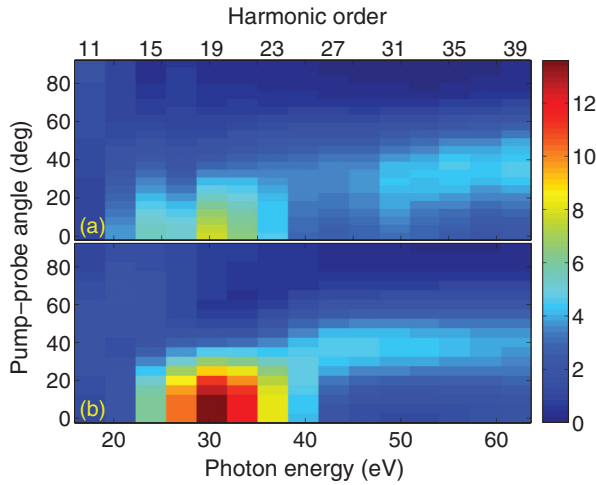


FIG. 3. (Color online) (a) Measured XUV intensity as a function of pump polarization angle and photon energy. (b) Calculated harmonic yield as a function of angle and photon energy using QRS theory. The calculations include HHG components parallel and perpendicular to the laser polarization vector. All the harmonic data are normalized to the corresponding values from an isotropic gas.

angle-dependent PICS of the $3\sigma_g$ HOMO of N_2 , which is dominated by a shape resonance and a Cooper-like minimum in the relevant energy range.

Briefly, within the QRS theory, the laser-induced dipole from a fixed-in-space molecule is the product of a target-independent returning electron wave packet and the field-free photo-recombination dipole. We simulate the former using the strong-field approximation (SFA) and calculate the latter with a state-of-the-art molecular photoionization code (EPOLYSCAT) [31,32]. We coherently convolve the delay-dependent molecular axis distribution—obtained from the fitting procedure described above—with the angle-dependent induced dipole obtained from the QRS calculation. This procedure is detailed in Ref. [5].

The simulation results are shown in Fig. 2 with the experimental data for some harmonics. All the main features listed above regarding the variation in revival structure with harmonic order are reproduced by the theory. This includes the inversion of the $1/8$ th revival, which requires contributions from $n > 2$ terms. However, there are still some disagreements. First, calculation for H19 has been rescaled by a factor of 0.5 to match with the experiment at the revival peaks, although they agree quite well for the intermediate time delays without the rescaling. Second, the situation is opposite for H31, where the QRS calculation underestimates the yield for intermediate time delays, although it agrees relatively well near the revival peaks. Those two harmonics appear to be at the center of the shape resonance and Cooper-like minimum of the theoretical PICS, respectively, as can be seen in panel (a) of Fig. 3. Compared to the experiment, QRS overestimates both features. One possible reason is that calculation is performed for a single molecule, while in the experiment there are harmonics emitted by different molecules at different initial phases in the interaction region, which may wash out both features to some extent.

III. ANGLE-DEPENDENT HARMONIC YIELDS: DIRECT OBSERVATION OF THE SHAPE RESONANCE AND COOPER MINIMUM

The angle dependence of HHG was also probed directly by rotating the pump polarization—and hence the molecular axis distribution—in 90 steps of 4° each with the probe arriving at the full revival (~ 12.5 ps). The yield for every harmonic was normalized to that from unaligned molecules and is shown in Fig. 3(a). The most striking feature is the presence of a strong and quite broad peak near 30 eV at angles below 40° . Interestingly, the HHG yield is peaked at small angles only for harmonics below H25 (or $E \leq 40$ eV). The peak shifts to $\sim 40^\circ$ as energy increases to 65 eV. This is in contrast to the earlier experimental data [33,34] measured with weaker alignment, where the alignment dependence of HHG yields was seen to be nearly unchanged with harmonic orders and peaks at small angles for most observed harmonics. The observed features are reproduced well in a QRS calculation, shown in Fig. 3(b), although the theory overestimates HHG yields near 30 eV by nearly a factor of two. By using QRS, the dominant peak near 30 eV can be attributed to a $3\sigma_g \rightarrow k\sigma_g$ shape resonance [31,35]. The calculation also shows a clear minimum at small angles near 52 eV, which is associated with a minimum near 50 eV in the PICS [see Jin *et al.* [35] and Fig. 4(a)]. We have found that this minimum is nearly invisible in the QRS calculation with weaker alignment ($\langle \cos^2 \theta \rangle < 0.65$). Interestingly, this minimum can also be seen in the experimental data, although it is shallower than the theoretical result and occurs near 58 eV. We note that such a minimum has been observed quite recently by Bertrand *et al.* [23] by using a 1200-nm laser. Their 800-nm data showed a much weaker minimum as compared to the mid-IR case. To

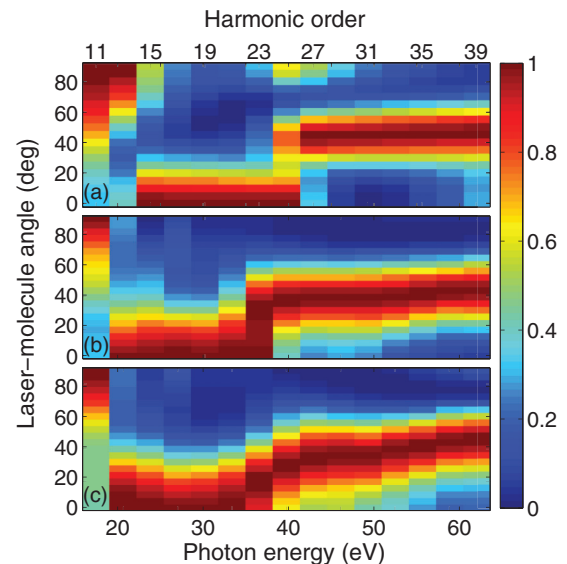


FIG. 4. (Color online) (a) Theoretical molecular-frame differential PICS of the HOMO (the PICS which are responsible for both parallel and perpendicular components of HHG are included); (b) and (c) PICS retrieved from the experimental angle and delay scans, respectively. All results are normalized to peak value for each harmonic order individually. See text for details of retrieval procedures.

our knowledge, this is the first time that signatures of both the shape resonance and the Cooper-like minimum have been seen directly in harmonic measurements in the laboratory frame. We further note that the minimum observed by Bertrand *et al.* [23] at 42 eV is in better agreement with our theoretical result than the present experimental data.

IV. EXTRACTING ANGLE-DEPENDENT PICS FROM BOTH DELAY AND ANGLE SCANS

In order to extract the PICS, we first deconvolve the molecular-frame HHG from the measured angle scan. Our fitting procedure is essentially the same as that of Ref. [23], and we do not detail it here. We do, however, point out that the two approximations used—neglecting the angle dependence of the phase when the molecules are confined to a narrow cone and the use of the perpendicular component of the molecular-frame dipole in lieu of the component perpendicular to both the laser polarization and propagation axes—are both better justified for our tightly aligned molecules. The extracted molecular-frame HHG results are then divided by the ionization rate obtained from a separate experiment in which angle- and delay-dependent yields of N_2^+ ions are measured and a similar fitting algorithm is used to get the molecular-frame ionization rate (details of the experiment will be reported elsewhere). The third factor in the QRS theory—the target-independent returning electron wave packet—is not directly accessible in the experiment, and the detection efficiency of the XUV spectrometer is also not calibrated. To remove the effects of these factors, the data for each harmonic is normalized to its peak value.

Since the angle dependence of the HHG signal is available from the fitting procedure for the delay scans as well, we can extract the PICS from that data too and compare both with theoretical one calculated with EPOLYSCAT [4,31,32,35]. In the theoretical calculation, the recombination dipole component responsible for HHG polarized perpendicular to the laser polarization is included. With the normalization, this addition does not change the results significantly. All three are shown in Fig. 4. We can see very good overall agreement both between the two experimental results, and between either and theory. It is also obvious that, due to the high degree of alignment, even the raw angle-scan data [Fig. 3(a)] shows very clear signatures of all the main features of the molecular frame. The angle dependence obtained from the fitting procedure for the delay scans described above is shown in Fig. 4(c), which

shows relatively good agreement with the theoretical PICS in Fig. 4(a). We note that the assumption of angle-independent phase is not as well justified here as in the case of the angle scan at peak alignment since the delay-dependent angular distribution is often quite broad. The good agreement between the two extraction results suggests that in the time delay fitting the dominant contribution for each harmonic still comes from a narrow range of angles. Experiments that measure both phase and amplitude of the harmonics as a function of angle or delay will be necessary for better determination of PICS, although so far such measurements have not employed a high degree of alignment.

V. CONCLUSIONS

These results further cement the emergence of HHG as a viable tool for broadband (inverse) photoionization measurements in the molecular frame. In particular, we showed that such inversion can be done without *any* prior knowledge of the molecular structure and thus has the potential to reveal new molecular-frame features. Furthermore, the time resolution of such measurements could be extended to the sub-femtosecond domain by using techniques that have been developed for attosecond pulse generation, wherein HHG is restricted to a small fraction of a single optical cycle. The successful retrieval of the PICS from pump-probe delay scans also points to the route to extending this method to asymmetric top molecules. The orientation of such molecules with respect to the laser polarization vector must be specified in terms of two Euler angles, and the rotational wave packet launched by the alignment pulse is rather complex and also involves both angles. Yet, by fitting the revival structure of different harmonics to a series of Wigner matrix elements, it should be possible to extract the fully differential PICS with dependence on two angles. It will likely be necessary to measure the harmonic phase and to disentangle the contributions of lower lying orbitals, but these issues are already being addressed experimentally. HHG could complement molecular-frame time-resolved photoelectron angular distribution measurements in energy and temporal regimes that would be very challenging for conventional techniques.

ACKNOWLEDGMENT

This work was supported by the Chemical Sciences, Geosciences, and Biosciences Division, Office of Basic Energy Sciences, Office of Science, US Department of Energy.

-
- [1] J. W. Gallagher, C. E. Brion, J. A. R. Samson, and P. W. Langhoff, *J. Phys. Chem. Ref. Data* **17**, 9 (1988).
 - [2] J. Itatani, J. Levesque, D. Zeidler, H. Niikura, H. Pépin, J. Kieffer, P. Corkum, and D. Villeneuve, *Nature (London)* **432**, 867 (2004).
 - [3] M. Lein, N. Hay, R. Velotta, J. P. Marangos, and P. L. Knight, *Phys. Rev. Lett.* **88**, 183903 (2002).
 - [4] A.-T. Le, R. R. Lucchese, S. Tonzani, T. Morishita, and C. D. Lin, *Phys. Rev. A* **80**, 013401 (2009).
 - [5] A.-T. Le, R. R. Lucchese, M. T. Lee, and C. D. Lin, *Phys. Rev. Lett.* **102**, 203001 (2009).
 - [6] J. L. Krause, K. J. Schafer, and K. C. Kulander, *Phys. Rev. Lett.* **68**, 3535 (1992).
 - [7] P. B. Corkum, *Phys. Rev. Lett.* **71**, 1994 (1993).
 - [8] O. Smirnova, Y. Mairesse, S. Patchkovskii, N. Dudovich, D. Villeneuve, P. Corkum, and M. Ivanov, *Nature (London)* **460**, 972 (2009).

- [9] B. K. McFarland, J. P. Farrell, P. H. Bucksbaum, and M. Gühr, *Science* **322**, 1232 (2008).
- [10] T. Kanai, S. Minemoto, and H. Sakai, *Nature (London)* **435**, 470 (2005).
- [11] S. Minemoto, T. Umegaki, Y. Oguchi, T. Morishita, A.-T. Le, S. Watanabe, and H. Sakai, *Phys. Rev. A* **78**, 061402 (2008).
- [12] K. Yoshii, G. Miyaji, and K. Miyazaki, *Phys. Rev. Lett.* **101**, 183902 (2008).
- [13] X. Zhou, R. Lock, N. Wagner, W. Li, H. C. Kapteyn, and M. M. Murnane, *Phys. Rev. Lett.* **102**, 073902 (2009).
- [14] H. J. Wörner, H. Niikura, J. B. Bertrand, P. B. Corkum, and D. M. Villeneuve, *Phys. Rev. Lett.* **102**, 103901 (2009).
- [15] P. M. Kraus, A. Rupenyan, and H. J. Wörner, *Phys. Rev. Lett.* **109**, 233903 (2012).
- [16] A. Rupenyan, J. B. Bertrand, D. M. Villeneuve, and H. J. Wörner, *Phys. Rev. Lett.* **108**, 033903 (2012).
- [17] S. Baker, J. S. Robinson, C. A. Haworth, H. Teng, R. A. Smith, C. C. Chirila, M. Lein, J. W. G. Tisch, and J. P. Marangos, *Science* **312**, 424 (2006).
- [18] W. Li, X. Zhou, R. Lock, S. Patchkovskii, A. Stolow, H. C. Kapteyn, and M. M. Murnane, *Science* **322**, 1207 (2008).
- [19] H. J. Wörner, J. B. Bertrand, D. V. Kartashov, P. B. Corkum, and D. M. Villeneuve, *Nature (London)* **466**, 604 (2010).
- [20] H. J. Wörner, J. B. Bertrand, B. Fabre, J. Higuët, H. Ruf, A. Dubrouil, S. Patchkovskii, M. Spanner, Y. Mairesse, V. Blanchet *et al.*, *Science* **334**, 208 (2011).
- [21] K. Yoshii, G. Miyaji, and K. Miyazaki, *Phys. Rev. Lett.* **106**, 013904 (2011).
- [22] A. D. Shiner, B. E. Schmidt, C. Trallero-Herrero, H. J. Wörner, S. Patchkovskii, P. B. Corkum, J. C. Kieffer, F. Légaré, and D. M. Villeneuve, *Nat. Phys.* **7**, 464 (2011).
- [23] J. B. Bertrand, H. J. Wörner, P. Hockett, D. M. Villeneuve, and P. B. Corkum, *Phys. Rev. Lett.* **109**, 143001 (2012).
- [24] U. Even, J. Jortner, D. Noy, N. Lavie, and C. Cossart-Magos, *J. Chem. Phys.* **112**, 8068 (2000).
- [25] J. P. Farrell, B. K. McFarland, P. H. Bucksbaum, and M. Gühr, *Opt. Express* **17**, 15134 (2009).
- [26] J. Mikosch, C. Z. Bisgaard, A. E. Boguslavskiy, I. Wilkinson, and A. Stolow, *J. Chem. Phys.* **139**, 024304 (2013).
- [27] S. Ramakrishna and T. Seideman, *Phys. Rev. Lett.* **99**, 113901 (2007).
- [28] R. M. Lock, S. Ramakrishna, X. Zhou, H. C. Kapteyn, M. M. Murnane, and T. Seideman, *Phys. Rev. Lett.* **108**, 133901 (2012).
- [29] F. Rosca-Pruna and M. J. J. Vrakking, *J. Chem. Phys.* **116**, 6579 (2002).
- [30] T. Morishita, A.-T. Le, Z. Chen, and C. D. Lin, *Phys. Rev. Lett.* **100**, 013903 (2008).
- [31] R. R. Lucchese, G. Raseev, and V. McKoy, *Phys. Rev. A* **25**, 2572 (1982).
- [32] R. E. Stratmann and R. R. Lucchese, *J. Chem. Phys.* **102**, 8493 (1995).
- [33] J. Itatani, D. Zeidler, J. Levesque, M. Spanner, D. M. Villeneuve, and P. B. Corkum, *Phys. Rev. Lett.* **94**, 123902 (2005).
- [34] A. Scrinzi, M. Y. Ivanov, R. Kienberger, and D. M. Villeneuve, *J. Phys. B* **39**, R1 (2006).
- [35] C. Jin, J. B. Bertrand, R. R. Lucchese, H. J. Wörner, P. B. Corkum, D. M. Villeneuve, A.-T. Le, and C. D. Lin, *Phys. Rev. A* **85**, 013405 (2012).